Korean J. Chem. Eng., 40(2), 419-428 (2023)
DOI: 10.1007/s11814-022-1314-x

pISSN: 0256-1115
eISSN: 1975-7220

Novel silicatein-like protein for biosilica production from *Amphimedon queenslandica* and its use in osteogenic composite fabrication

Mi-Ran Ki[*,], Ki Sung Park[*], Mohamed A. A. Abdelhamid[*,***], and Seung Pil Pack[*,†]**

*Department of Biotechnology and Bioinformatics, Korea University, Sejong 30019, Korea
**Institute of Industrial Technology, Korea University, Sejong 30019, Korea
***Department of Botany and Microbiology, Faculty of Science, Minia University, Minia 61519, Egypt
(*Received 31 July 2022 • Revised 7 October 2022 • Accepted 8 October 2022*)

Abstract−Efforts to find sustainable and eco-friendly ways to conduct chemical reactions have led to the mimicking of nature. In this study, a new silica polymerization protein that can produce silica in an environmentally friendly manner was developed using cathepsin L-like protein (AqCtL) from *Amphimedon queenslandica* with a 61% sequence identity to that of silicatein-alpha, which is a natural biosilicifying enzyme. To stabilize the protein structure, heterologously expressed AqCtL in *Escherichia coli* was mutated into AqCtLSN by changing the amino acid residues responsible for protease cleavage. The insoluble form of AqCtLSN was reconstituted into a soluble protein through the refolding process, displaying silica-condensing activity from silicic acid. AqCtLSN self-assembled, aggregated, and attached to a support in the PBS buffer without losing silica deposition activity. These properties were applied to fabricate a silica-hybrid material using a gelatin-tyramine-alginate cross-linked hydrogel as a scaffold. FT-IR analysis revealed that a silica hybrid material was produced owing to the in situ silicification by AqCtLSN immobilized on the hydrogel. The surface of biosilica mediated by AqCtLSN demonstrated an increase in cell proliferation, alkaline phosphatase activity, and calcium mineral precipitation in the osteogenesis of MC3T3 E1 cells compared to those without biosilica. In conclusion, AqCtLSN, recombinantly expressed in *E. coli*, is a novel biosilica-forming protein that can be used to produce composites for biomedical applications, especially bone regeneration.

Keywords: Cathepsin L, Silicatein, Biosilicification, Biosilica Composite, Bone Regeneration

INTRODUCTION

Biomineralization is a process by which organisms receive inorganic substances from the environment and create organic/inorganic composite structures using a well-controlled biological system [1]. Organisms create multidimensional inorganic skeletons, such as calcium carbonate, calcium phosphate, silica, and iron oxide, in an aqueous solution under ambient conditions from simple inorganic precursors using organic materials, such as proteins, lipids, and carbohydrates [2-6]. Ever since organic molecules and the mechanisms involved in biomineralization have been discovered, new synthetic alternatives for materials of interest developed on the basis of biomineralization have been attempted, yielding the synthesis of organic-inorganic composites, ranging from the nano-level to macro-level in an environmentally friendly manner [7-9].

The biological formation of amorphous hydrated silica, referred to as biosilicification, occurs in a variety of organisms, including diatoms, sponges, mollusks, and higher plants [2]. The biosilicification mechanism in diatoms and sponges has been gradually uncovered through the discovery of silaffin and silicatein proteins, respectively [2,10]. Additionally, biomolecules, including silaffin and silicatein, as well as biomimetic silica-forming molecules have been widely studied to innovatively design a variety of silica-based materials [11]. Silica is an industrial material with a wide range of applications [12], and its non-toxic and highly biocompatible properties make it suitable for biomedical, biosensor, and optical applications [13,14]. Silica-based porous structures are advantageous for removing pollutants from the environment [15,16]. However, a combination of high temperature and extreme pH is required for the conventional chemical synthesis of silica [17,18]. Therefore, inspired by nature, studies on fabricating silica composite materials under eco-friendly conditions have gained attention in materials science [19]. In general, organic molecules involved in silica formation self-assemble to form a matrix or nucleus, thereby serving as a self-template on which silica minerals precipitate to form a mineral structure. Therefore, they function not only as catalysts but also as biomineral ingredients [20,21]. The availability of organic catalysts is thus a prerequisite for designing novel silica composites inspired by nature, because the amount of organic catalysts isolated from natural sources is limited [22]. For proteins, this can be achieved using recombinant protein technology.

Silicatein, a general catalyst for the synthesis of silica skeletons, such as spicules in siliceous demosponges [23-25], has been heterologously expressed in *E. coli* and used for various applications [26-28]. To apply biosilica to the industrial field, the intellectual property of organic molecules (catalyst) for biosilicification must be considered. Therefore, studies on developing novel silica-catalyzing proteins and improving existing proteins to usable proteins are in progress [22,29,30].

Silicatein α has a cDNA sequence that is highly similar to that

†To whom correspondence should be addressed.
E-mail: spack@korea.ac.kr

of cathepsin L protein [2]. Cathepsin L belongs to the family of papain-like peptidases with a catalytic triad of cysteine, histidine, and asparagine [31]. The main difference between silicatein and cathepsin L is the replacement of cysteine with serine in the catalytic triad [2]. Based on gene-level analysis, Muller et al. suggested that silicatein and cathepsin L in the phylum Porifera evolved from a common ancestor of cysteine proteases and that the modification of the first amino acid among the catalytic triad is a suitable target for the chemical modulation of the enzyme function of silicatein or cathepsin [22,32]. By changing certain residues, cathepsin L is considered the best alternative candidate for engineered silica-catalyzing proteins [22,30,33,34].

In this study, a novel protein was selected using the Basic Local Alignment Search Tool (BLAST) with amino acid sequences of silicatein-alpha (SdSiA) from *Suberites domuncula* as a query against a protein database to obtain an improved silica-polymerizing protein from cathepsin L. The novel protein (AqCtLSN) produced recombinantly in *E. coli* was investigated for its ability to deposit silica and its usability in the fabrication of silica hybrid materials.

EXPERIMENTAL SECTION

1. Materials

Escherichia coli (*E. coli*) DH5α (competent cells, Thermo Fisher Scientific Korea, Seoul, Korea) was used as the host for plasmid cloning, and *E. coli* BL21 (DE3) (Agilent Technologies, Santa Clara, CA) was used as the host for protein expression. The pET42b+ expression vector was obtained from Novagen (Madison, WI). Tetramethyl orthosilicate (TMOS), tetraethyl orthosilicate (TEOS), porcine gelatin (Type A), alginic acid sodium salt from brown algae, tyramine, p-nitrophenyl phosphate liquid substrate system, choline chloride·HCl, ascorbic acid, β-glycerophosphate, and Alizarin Red-S were purchased from Sigma-Aldrich (St. Louis, MO, USA). Urea and hydrogen peroxide were purchased from Samchun Chemical Co. Ltd. (Seoul, Korea). Horse radish peroxidase (HRP) was purchased from Worthington Biochemical Co. (Lakewood, NJ, USA). All other reagents used were of analytical grade.

2. Construction of Expression Vector

The cDNA sequences of a predicted cathepsin L1-like protein from *Amphimedon queenslandica* (GenBank ID: XP_003383726.1) were optimized for expression in *E. coli* [9] and synthesized by Genscript (Seoul, Korea). The cDNA fragment for the mature form of this protein, designated as AqCtL, was amplified by PCR using forward [5-ggaattcCATATG CCGGAAGAAGTTGACTGGCGCA-3 (underlined: *Nde*I site)] and reverse [5-ccgAAGCTT CAGCGTCGGGAAGCTGGCCGC-3 (underlined: *Hin*dIII site)] primers. The *Nde*I/*Hin*dIII-digested DNA fragments were cloned into a likewise-digested pET42b+ vector to create pET-AqCtL, which has an 8×His tag at the C-terminus. Mutation of AqCtL was performed by site-directed mutagenesis using a combination of PCR with Pfu DNA polymerase and *Dpn*I restriction enzyme digestion, according to the manufacturer's instructions (Thermo Fisher Scientific Inc. Rockford, IL, USA) [35] using pET-AqCtL as a template and forward [5-CAGGCTCTGTCGAATGACAAACTGGTTCACCTGA-3, (underlined: mutation site)] and reverse [5-CAGTTTGTCATTCGACAGAGCCTGTGCACCTTCCAGT-3, (underlined: mutation site)] primers. Mutations in the residues of both A41H42 were used to produce the A41S/H42N mutant designated as AqCtLSN. Mutant DNA sequences were confirmed by gene sequencing analysis (Cosmo Genentech, Seoul, Korea). For silicatein expression, we used a previously constructed vector named pET-SIL [28] and produced a recombinant protein designated as SdSiA.

3. Expression and Purification of the Recombinant Proteins

E. coli BL21 (DE3) harboring pET-AqCtL, pET-AqCtLSN, or pET-SIL was grown in Luria broth (LB) supplemented with kanamycin (25 μg mL^{-1}) at 37 °C to an absorbance (A_{600}) of 0.4-0.6, followed by the addition of isopropyl-β-D-thiogalactoside (IPTG; 0.1 mM) and then additionally incubated overnight at 20 °C. The cell pellet obtained from 200 mL of culture broth was suspended in 10 mL of 50 mM Tris-HCl, 300 mM NaCl, and 1% glycerol (pH 8.0). The bacterial suspensions were broken by sonication using a Branson Digital Sonifer-250 (Danbury, CT) fitted with a 9.5-mm tip (amplitude: 50%, 1 s pulse/5 s pause for 5 min on ice). The broken cells were centrifuged at 13,000 rpm for 30 min at 4 °C to obtain insoluble fraction. The resulting precipitate was washed thrice with 1% of Triton 114 followed by washing with ddH_2O, and lyzed in 50-mM Tris-HCl, 300-mM NaCl containing 7 M urea. The solubilized proteins were purified using HisPurTM cobalt resin (Thermo Fisher Scientific Korea Ltd. Seoul, Korea) under denatured conditions. The proteins were analyzed using sodium dodecyl sulfate-polyacrylamide gel electrophoresis (SDS-PAGE).

4. Refolding of the Recombinant AqCtLSN

The denatured AqCtLSN was reconstituted as described by Elkhooly et al. [36]. The purified denatured protein in 7 M urea was delivered at a flow rate of 0.5 $mLmin^{-1}$ into the first refolding buffer constituting 50 mM Tris-HCl (pH 9.0), 0.5 M L-arginine, 9 mM GSH, 1 mM GSSG, 0.3 M NaCl, and 1 mM KCl, yielding a 10-fold dilution. The diluted solution was double concentrated with an Amicon Ultra centrifugal filter with a 10 kDa cut-off (Merck Millipore), which was transferred with the same flow rate as aforementioned into the second refolding buffer comprising 50 mM Tris-HCl (pH 9.0), 0.5 M L-arginine, 0.3 M NaCl, and 1 mM EDTA. This procedure was repeated four more times to dilute the urea concentration to less than 10 mM. The resulting 10 mL solution was dialyzed against 1 L of the third refolding buffer containing 50 mM Tris-100 mM glycine (pH 9.0) for 24 h. If required, it was used after the final dialysis against 50 mM Tris-HCl (pH 8.0) or PBS. All processes were carried out at 4 °C. The protein concentration was determined using the Bradford assay (Thermo Fisher Scientific).

5. Silica Deposition

The silica polymerization activity was initiated by adding 100 μL of 1 M hydrolyzed TEOS to 1 mL of 50 mM Tris-HCl (pH 8.0) or 20 μL of 1 M hydrolyzed TMOS to 1 mL of 50 mM sodium phosphate buffer containing 10% sucrose (pH 7.5) in the presence of solubilized AqCtLSN. The reaction was performed overnight for 6 h at 25 °C with vigorous shaking. In the control assay, equivalent amounts of bovine serum albumin (BSA), SdSiA, or no protein were added to the reaction mixture. Silica deposition was measured based on the modified molybdenum blue method as previously described [28].

6. Silica Quantification

The amount of dried silica synthesized by AqCtLSN was deter-

mined using the modified molybdenum blue method described previously [37].

7. Preparation of Biosilica/Gelatin-alginate-tyramine Hydrogel

Gelatin or sodium alginate powder (0.3 g) was dissolved in 30 mL of 50 mM 2-(N-morpholino) ethanesulfonic acid) (MES) buffer, followed by incubation for 1 h at 60 °C. After cooling to room temperature, 0.25 g of tyramine hydrochloride, 0.15 g, 1-Ethyl-3-[3-(dimethylamino)propyl]carbodiimide (EDC), and 0.06 g of N-hydroxysuccinimide (NHS) were added to the gelatin or alginate solution. After the pH was adjusted to 5.3, the mixture was stirred overnight at room temperature. Thereafter, the reactant was dialyzed against ddH_2O until no tyramine was detected in the dialysate at 275 nm. After dialysis, tyramine-conjugated gelatin (GT) or tyramine-conjugated alginate (ALT) solution was freeze-dried. Either lyophilized GT or ALT was dissolved at a concentration of 1% in PBS, and then GT and ALT were mixed together with same volume to obtain 10 mL to which 10 units of horse radish peroxidase (HRP) per mL and H_2O_2 at a final concentration of 5 mM were added to induce gelation. The as-prepared hydrogel was dialyzed against PBS for one day in the presence or absence of 1 $mgmL^{-1}$ AqCtLSN to allow AqCtLSN to bind to the hydrogel, and then dialyzed against ddH_2O for another day. The dialyzed hydrogel was either used immediately or stored after freeze-drying. For silica mineralization of as-prepared hydrogel, dried gel block was immersed in a mixture of 1.5% hydrolyzed TEOS (v/v), 36 mM choline chloride, and 46% ethanol (v/v), designated as 1.5% silicic acid [38,39], and left to stand for one day to induce in situ silica deposition.

8. Preparation of Culture Plate Coated with Biosilica/GT/ALT

Prior to the cell culture work, a mixture of 0.5% GT and 0.5% ALT in PBS was overlaid onto wells of a 96-well plate, a crosslinking reaction was induced by adding HRP and H_2O_2; the solution was left to settle overnight, and the sediments were left to dry at the bottom of a well under air stream in a biosafety cabinet (BSC). The dried film on the plate was washed thrice with ddH_2O. To incorporate AqCtLSN into gel film, 0.01% AqCtLSN was overlaid on the gel surface, and the solution was left to settle and to be absorbed. To precipitate silica in situ on the coated plate surface, 1.5% silicic acid solution was placed on a well plate and left for one day to induce silica mineralization. After reactants that did not participate in the reaction were removed, the plate was washed with distilled water and dried. For sterilization of the aforementioned materials, 70% ethanol was overlaid on the plate for one hour or more. The plated cells were washed with sterile distilled water thrice and dried overnight on a BSC.

9. Chemical and Physical Structure of As-prepared Biosilica/GT/ALT

The prepared hydrogel and its silica mineralized form were analyzed using scanning electron microscopy (SEM) (FE-SEM, JSM-6700F, JEOL, Japan) and a high-vacuum Fourier-transform infrared spectroscopy (FT-IR)/Raman imaging spectrometer system (KBSI, Busan, Korea).

10. MC3T3 E1 Cell Culture

Mouse preosteoblast MC3T3 E1 subclone 4 (ATCC® CRL-2593™) was purchased from ATCC (Manassas, VA, USA). Passage 15 cells were cultured in a growth medium (GM) composed of minimal essential medium alpha (MEM-α, Hyclone™, Citiva Korea) supplemented with 10% fetal bovine serum (HyClone™ FBS) and 1% penicillin-streptomycin solution (Hyclone penicillin-streptomycin 100x solution) at 37 °C in a humidified atmosphere with 5% CO_2. For osteoblast differentiation, the GM was replaced with bone differentiation medium (BM) made from GM supplemented with 50 μg mL^{-1} L-ascorbic acid and 10 mM β-glycerophosphate. The BM was replaced every three days during the osteogenesis experiment.

11. Cell Proliferation

The MC3T3 E1 osteoblastic cells (1×10^4 cells/well) in GM were seeded onto the as-prepared well plates in 96-well plates. The cells were incubated at 37 °C in 5% CO_2 incubator for seven days. The culture medium was replaced every three days. The 3-(4,5-dimethylthiazol-2-yl)-5-(3-carboxymethoxyphenyl)-2-(4-sulfophenyl)-2H-tetrazolium (MTS) assay was performed to quantify cell proliferation using the CellTiter 96® Aqueous One Solution Cell Proliferation Assay Kit (Promega) according to the manufacturer's instructions. The reaction solution was transferred to a new 96 well plate and absorbance was measured at 490 nm using a UV/visible microplate reader (Infinite M200 PRO NanoQuant; TECAN) [40].

12. Alkaline Phosphatase (ALP) Activity

The MC3T3 E1 cells were cultured in GM for seven days under the same conditions as mentioned above, and the medium was replaced with BM to induce osteogenesis. The BM was replaced every three days, and 14 days after BM cultivation, ALP activity was determined using a p-nitrophenyl phosphate (pNPP) liquid substrate system (Sigma-Aldrich). The cells were washed with PBS and lyzed with 50 μL of PBS containing 1% Triton X-100 at 37 °C for 5 min, followed by adding 50 μL pNPP solution. The mixture was incubated at 37 °C for 10 to 30 min, depending on color development. Optical density was measured at 405 nm using a UV/visible microplate reader (Infinite M200 PRO NanoQuant; TECAN).

13. Calcium Deposition and Quantification

Calcium deposition was determined on the 21st day after cultivation of MC3T3 E1 cells in BM for osteogenic differentiation using the Alizarin Red S assay. The cells were washed twice with PBS without Ca^{2+} and Mg^{2+}, fixed in 4% paraformaldehyde in PBS for 30 min, rinsed with ddH_2O three times to remove phosphate ions, and then stained with 40 mM Alizarin Red-S aqueous solution at pH 4.2 for 15 min. The stained cells were rinsed with ddH_2O three times and dried. The cells were observed under a phase contrast microscope and then de-stained with 10% acetic acid for 30 min, and neutralized with 10% ammonium hydroxide [41]. The absorbance of the solubilized calcium extracts was determined at 562 nm using a UV/visible microplate reader (Infinite M200 PRO NanoQuant; TECAN).

14. Statistical Analysis

All values are presented as mean±SD. Statistical analyses were performed using Student's *t*-test. Statistical significance was set at * $P<0.05$, ** $P<0.01$, and *** $P<0.001$.

RESULTS AND DISCUSSION

1. Expression of AqCtL and its Mutant AqCtLSN

A predicted cathepsin L1-like protein of *Amphimedon queen-*

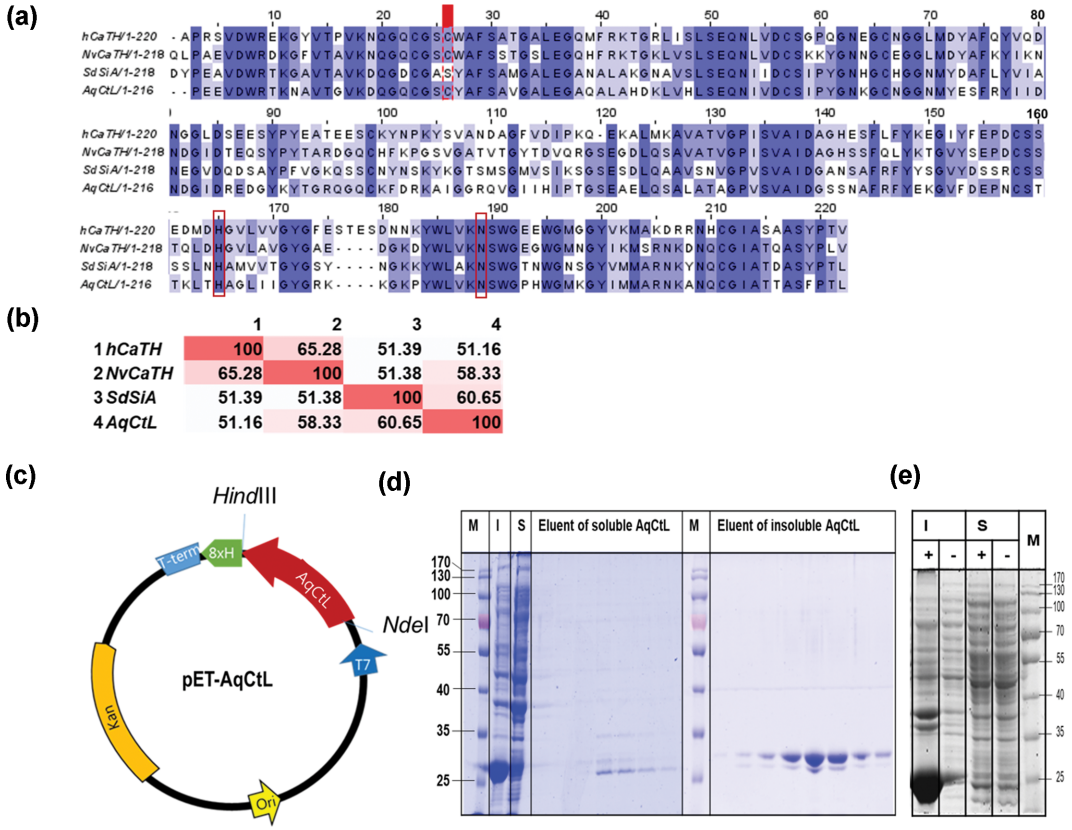

Fig. 1. Expression of recombinant AqCtL in *E. coli* BL21 (DE3). (a) AqCtL aligned with human cathepsin (hCaTH; PDB 3HHA), cathepsin L form *Nematostella vectensis* (NvCaTH; XP_001638528.1), and the SdSiA (AJ272013.1) using Clustal W (www.ebi.ac.uk). The catalytic triad amino acids, Cys26 or Ser26, His165 and Asn189 are marked with a red line box. (b) Percent identity matrix among proteins created by Clustal2.1. (c) Vector map of AqCtL (d) SDS-PAGE analysis of the expressed AqCtL. (e) SDS-PAGE analysis of the expressed AqCtL "I" and "S" indicating insoluble and soluble fractions, respectively by centrifugation of *E. coli* lysates. "+", or "-" indicates 0.1 mM IPTG addition for inducing of target protein. The SDS-profiles of the eluate purified according to the purification method of natural or non-natural His tagged protein depending on the solubility of protein are also shown.

slandica, a type of demosponge (GenBank ID: XP_003383726.1), was selected through a BLAST search of amino acid sequences of silicatein α from *Suberites domuncula*, a type of demosponge [23], as a query against the protein database. The cDNA sequences encoding AqCtL comprising 216 amino acids which is the mature protein form processed from full-length pre-pro cathepsin L1-like protein of *Amphimedon queenslandica* was deduced from both InterPro analysis (https://www.ebi.ac.uk/interpro) and the alignment with the sequences of silicatein α (SdSiA) from *Suberites domuncula*. The amino acid sequences of AqCtL shared 60.65% identity and 76.4% similarity with those of SdSiA, according to Clustal W program (www.ebi.ac.uk) (Fig. 1(a)). AqCtL displayed higher identity with SdSiA than cathepsin L either from human (hCaTH) (51.16%) [30] or *Nematostella vectensis* (NvCaTH) (58.33%) [22] (Fig. 1(b)). A cysteine residue rather than serine was present at the active site, indicating that this protein is a cathepsin L-like protein, whereas the ability to deposit silica and its high sequence similarity to that of SdSiA suggests that it is a silicatein-like protein [22,30,33]. As sponges are primitive multicellular aquatic animals constituting the phylum Porifera, to express sponge-derived proteins in *E. coli*, the gene encoding this protein was synthesized after converting the original cDNA sequences into codon usage bias of *E. coli* [42]. AqCtL was cloned into pET42b+ digested with *Nde*I and *Hin*dIII, which expresses a protein comprising 232 amino acids, including an open reading frame and an 8×histidine tag. Although the expression of the insoluble form was dominant over that of the soluble form in AqCtL, the soluble fraction demonstrated a similar band of AqCtL with a considerable amount on SDS-PAGE (Fig. 1(c)). In contrast, most of the SdSiA was expressed in the insoluble form, and the soluble fraction did not show a likely protein band regardless of IPTG induction (Fig. 1(d)). In terms of soluble protein expression, the AqCtL protein was heterologously expressed in *E. coli* BL21 (DE3) as a soluble protein with a higher yield than SdSiA (Fig. 1(c) and (d)). The two bands of AqCtL were observed by SDS-PAGE of the purified protein in both soluble and insoluble forms (Fig. 1(c)), possibly owing to autolysis and autocatalytic activity of AqCtL as a lysosomal protein [43]. To increase the structural stability of the protein, we first predicted where the protein was cleaved using the Signal P program (www.cbs.dtu.dk/services/SignalP) [44]. Analysis revealed a cleavage site between positions A41 and H42 (Fig. 2(a)). The amino acid residues in the likely positions of SdSiA represent A41 and K42. However, when the 42nd residue was replaced with K from H, the predicted cleavage site remained between positions A41 and K42 (Fig. 2(b)). There-

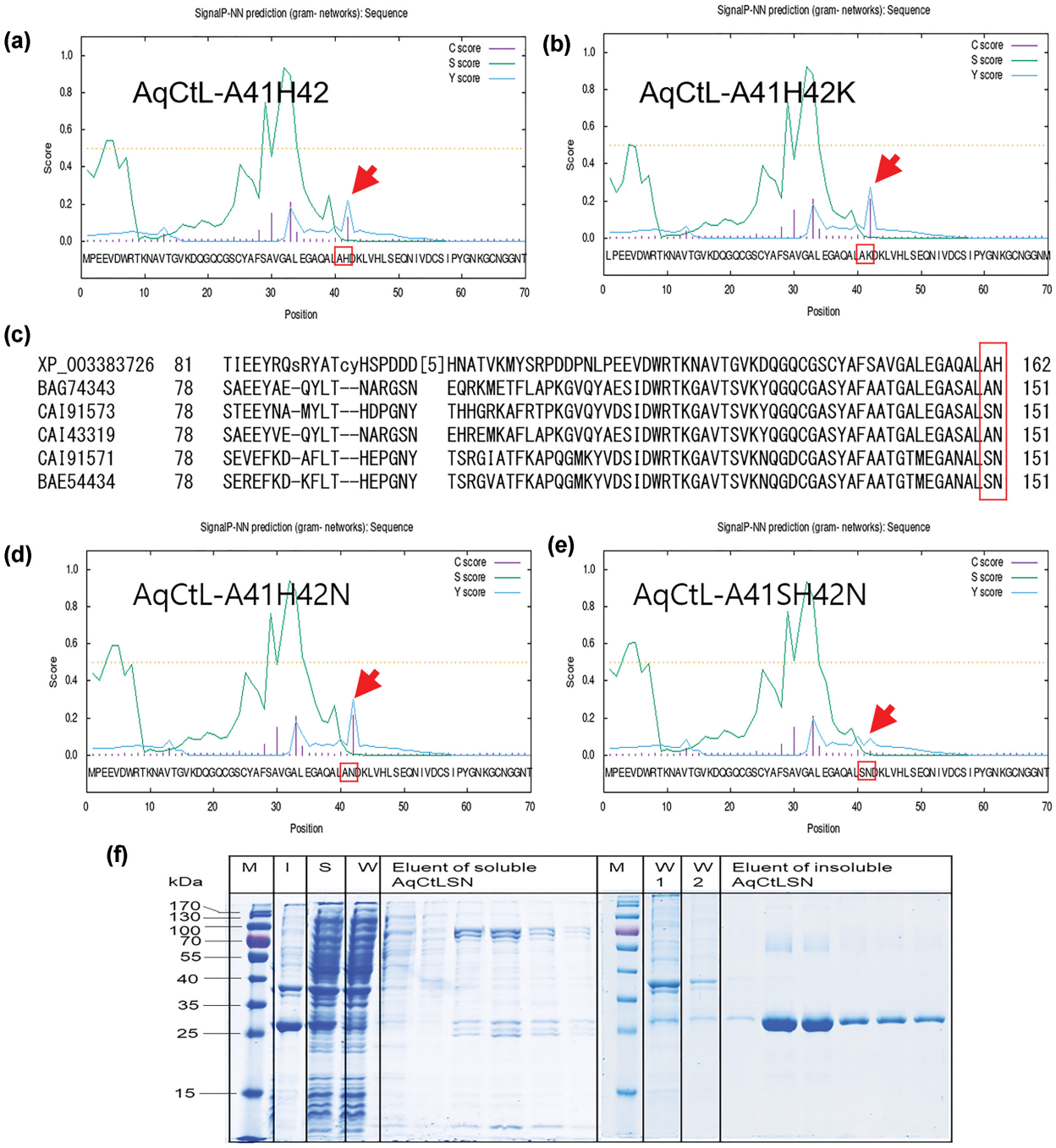

Fig. 2. Construction and expression of AqCtLSN. Predicted cleavage site of AqCtL was analyzed using Signal P 3.0 (a), which showed a cleavage between positions 41 and 42. The predicted cleavage site of the AqCtLH42K mutant displayed cleavage between positions 41 and 42 (b). The sequences of AqCtL (XP_003383726) were aligned with those of five types of silicatein (BAG74343 silicatein-M2 [*Ephydatia fluviatilis*], CAI91573.1 silicatein a4 [*Lubomirskia baicalensis*], CAI43319.1 silicatein alpha [*Lubomirskia baicalensis*], CAI91571.1 silicatein a2 [*Lubomirskia baicalensis*], and BAE54434.1 silicatein [*Ephydatia fluviatilis*]) (c). Sequence alignment was performed using the ClustalW software. The likely positions of A41 and H42 in AqCtL among silicateins are marked with a red column. Predicted cleavage sites of the mutants AqCtLH42N (d) and AqCtLA41SH42N (referred to as AqCtLSN later) (e). SDS-PAGE profile of AqCtLSN (f).

fore, we attempted to change the original amino acid residues to those that did not undergo cleavage. These residues were selected from the conserved sequences found in other silicateins by multiple alignment with that of AqCtL at the corresponding position (Fig. 2(c)). The 41st and 42nd amino acid residues A and H of AqCtL were changed to A, N, S, and N, respectively, and analyzed using the Signal P program. The cleavage probability decreased after changing to S41 and N42 (Fig. 2(d) and 2(e)). Therefore, A41 and H42

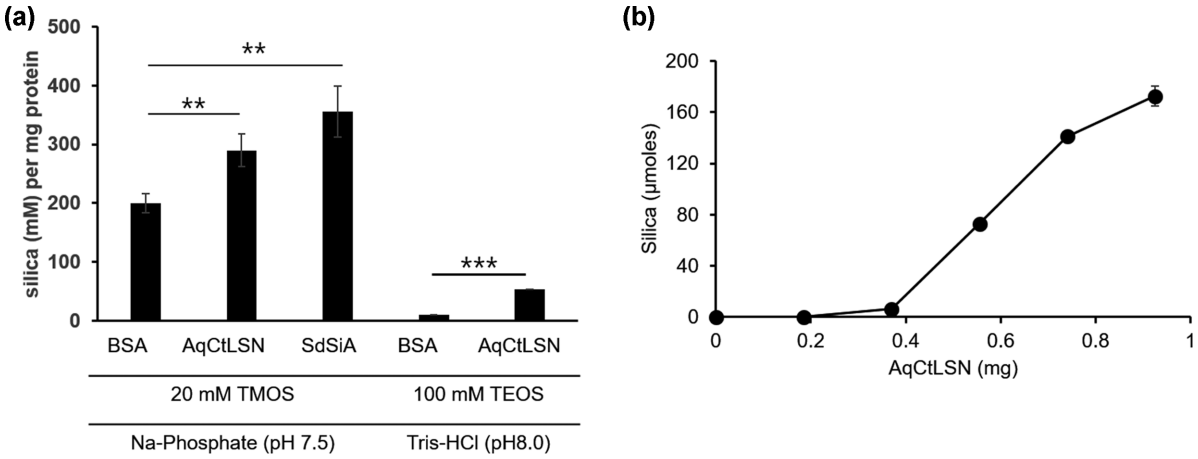

Fig. 3. Silica deposition activity. The specific silica deposition catalyzed by recombinant proteins was carried out using 100 mM hydrolyzed TEOS as substrate at 25 °C in 50-mM Tris-HCl (pH 8.0) or 20-mM hydrolyzed TMOS in 50-mM sodium phosphate buffer (pH 7.5) overnight. In the control assay, an equivalent amount of bovine serum albumin (BSA) was added to the reaction mixture. The silica deposition activity was expressed as the concentration (mM) of silica (SiO_2) produced per milligram of protein used (a). Silica formation rate using TEOS in Tris-HCl (pH 8.0) according to the amount of AqCtLSN (b). Values represent mean±standard deviation (SD) of three repeated experimental values. Asterisks indicate statistically significant differences (p<0.01, ***p<0.001 by the t-test).**

of AqCtL were mutated to S41 and N42, respectively. The purified protein band of the mutant, designated as AqCtLSN, yielded one band in SDS-PAGE for the insoluble protein (Fig. 2(f)). However, the soluble form of the protein was still degraded upon purification because of its protease activity, as in a previous study on hypothetical cathepsin-like protein from *Nematostella vectensis* [22]. Therefore, to produce a soluble protein in a stable form, further protein engineering is required. Hereafter, the refolded AqCtLSN from its insoluble form was used for the measurement of silica-forming activity and subsequent application of AqCtLSN.

2. Silica Deposition Activity of AqCtLSN in Soluble State

As mentioned in the Experimental section, AqCtLSN in the form of inclusion bodies was reconstituted in soluble form in 50-mM Tris-100 mM glycine buffer (pH 9.0). For the silica deposition reaction, solubilized AqCtLSN was dialyzed against 50-mM Tris-HCl (pH 8.0). The silica deposition ability of solubilized AqCtLSN was compared to that of SdSiA and BSA as positive and negative controls, respectively. In a phosphate buffer (pH 7.5) using TMOS as a silica precursor, AqCtLSN displayed significantly higher silica deposition specific activity (290±43.5 mM, $p<0.01$) than bovine serum albumin (BSA) did (200±16.4 mM), which was comparable to that of SdSiA (356±27.4, $p>0.05$ vs AqCtLSN) (Fig. 3(a)). BSA precipitated a significant amount of silica under these conditions owing to the large amount of cationic residues on the BSA surface [45]. However, when TEOS was used as the silica precursor at pH 8, the silica catalyzing activity of AqCtLSN (53.35±0.02 mM, $p<0.0001$ vs. BSA) increased more than five times that of BSA (10.28±0.29 mM), and the activity by BSA was the same as the blank value formed in buffer without any protein (data not shown), even though the total amount of silica deposition decreased compared to the reaction using TMOS. This indicates that silica deposition was catalyzed by AqCtLSN even without phosphate ions, similar to silicatein [29]. The silica formation rate using TEOS in Tris-HCl (pH 8.0), according to the amount of AqCtLSN, showed that approximately 188 μmoles of silica per mg of AqCtLSN was polymerized (Fig. 3(b)). Previously, it was shown that silicatein-like cathepsin L not only has protease activity, but also silica polymerization activity [22]. High amino acid sequence similarity to silicatein alpha, regardless of the catalytic triad, has demonstrated silica polymerizing activity in other studies as well [33,34]. According to Povarova et al., both silicatein A1 mutant, in which the serine residue is replaced with cysteine, and cathepsin mutant, in which the cysteine residue is replaced with serine, demonstrated increased silica deposition compared to the wild-type silicatein A1 [33].

3. Biosilica Coated Surface via AqCtLSN Protein Aggregates

When performing dialysis against PBS to change the buffer of 50 mM Tris-100 mM glycine in the AqCtLSN solution, we found that the protein thinly coats the inner surface of the dialysis membrane. The protein-coated dialysis membrane after freeze-drying was soaked in 1.5% silicic acid to check whether silica was formed on the surface of the dialysis membrane by the coated AqCtLSN. As shown in Fig. 4(A), the SEM image of the protein-coated dialysis membrane shows that the protein particles were aggregated and stacked like a fibril network. In the case of silica mineralization, silica was deposited on the AqCtLSN protein precipitation structure to form a fractal structure, in which silica particles of 300-400 nm were connected (Figs. 4(B) and 4(C)). The aggregation and sedimentation phenomena of AqCtLSN generally occur in SdSiA owing to its low solubility, and aggregation in aqueous media has been observed [21,29]. This aggregate protein demonstrated a highly adhesive property to glass cells [29]. We identified that AqCtLSN exhibits similar properties to SdSiA and attempted to use the filamentous aggregation and sedimentation behavior of AqCtLSN to attach it to other materials instead of glass cells to yield a silica composite through in situ silica deposition via AqCtLSN adhered to the surface. This reconstituted protein lacks a fixed or ordered three-dimensional structure, such as an intrinsically disordered protein (IDP) [46], and does not exhibit protease activity. Instead, because

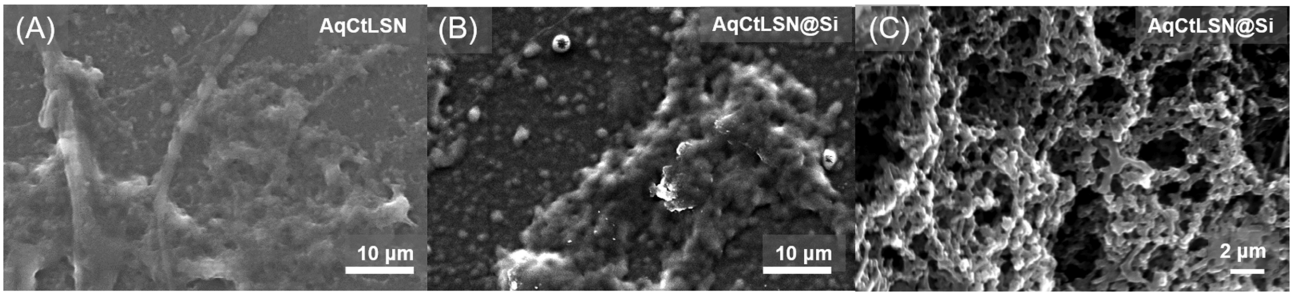

Fig. 4. SEM micrographs of AqCtLSN protein aggregates and its silica mineralization.

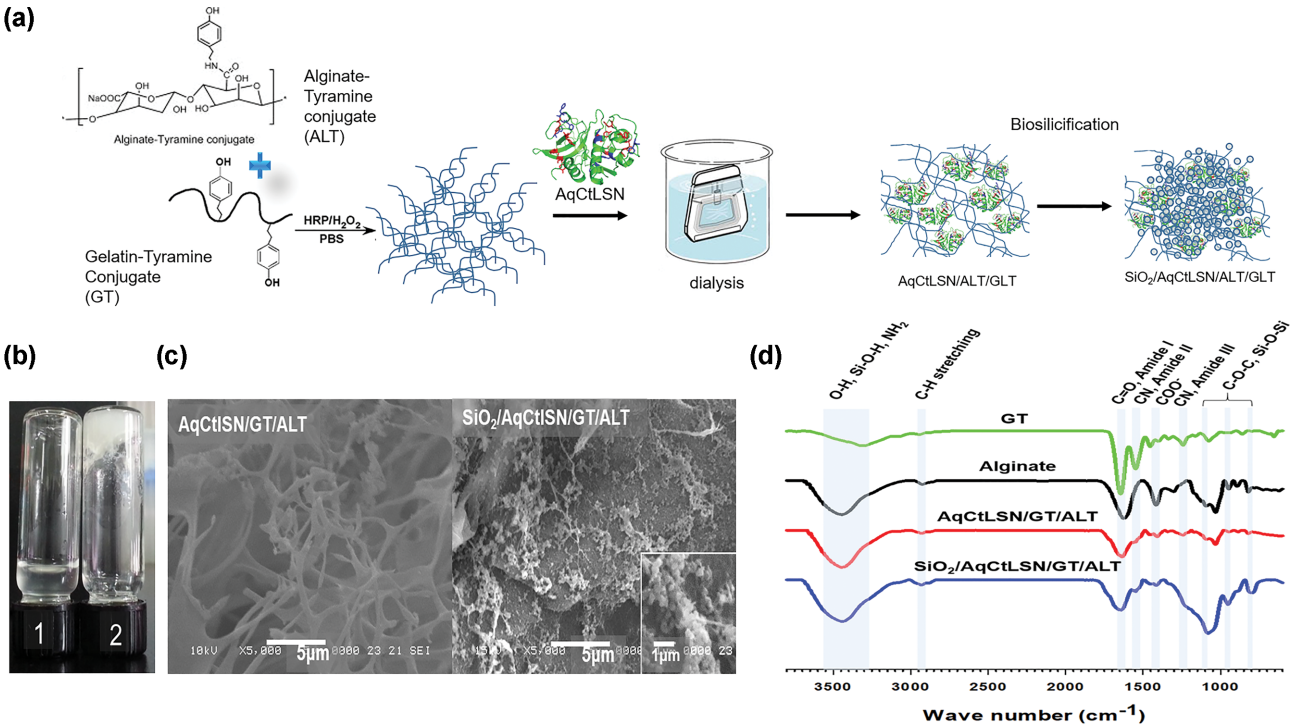

Fig. 5. Preparation of Si/AqCtLSN/GT/ALT. Schematic illustration of preparation of Si/AqCtLSN/GT/ALT (a). (b) GT/ALT solution before (1) and after (2) oxidation by HRP and H_2O_2. (c) SEM images of lyophilized AqCtLSN/GT/ALT and Si/AqCtLSN/GT/ALT. (d) Fourier transform infrared (FT-IR) spectra of GT, alginate, Si/GT/ALT, AqCtLSN/GT/ALT and Si/AqCtLSN/GT/ALT.

it is a positively charged protein (pI=8.4) under neutral conditions, it has the potential to self-assemble in the presence of phosphate ions, forming a protein template for mineral precipitation, such as that found in biomineralization by organisms [2,10,20,21].

4. Preparation of Biosilica Incorporated Hydrogel

To fabricate a biosilica-coupled composite for tissue engineering, the gelatin-alginate hydrogel was prepared by first linking tyramine to each polymer by an EDC/NHS reaction followed by covalent bridging between the two using HRP and H_2O_2-mediated oxidative coupling of the tyramine moiety, as shown in Fig. 5(a). A mixed solution of tyramine-conjugated gelatin (GT) and tyramine-conjugate alginate (ALT) remained in the liquid state and flowed when placed upside down (Fig. 5(b)-1). After a brief incubation with HRP and H_2O_2, the solution turned into a white gel, which did not flow when placed upside down (Fig. 5(b)-2). The cross-linked hydrogel was immersed in 50-mM Tris-100 mM glycine buffer containing 0.1% AqCtLSN solution and dialyzed against PBS to decrease the solubility of AqCtLSN by changing the buffer, which allowed the protein to bind to the gel surface. After soaking in 1.5% silicic acid overnight, washing with water, and drying, the FE-SEM observation revealed silica particles deposited on the surface shaped as a network comprising silica droplets (Fig. 5(c)). The chemical bonding of the composites was analyzed using FT-IR spectroscopy. FT-IR spectroscopy data showed typical amide I at ~1,660 cm^{-1} (C=O elongation), amide II at ~1,554 cm^{-1} (N-H variant), and amide III at ~1,240 cm^{-1} (the stretching bonds of C-H and bending bonds of N-H), confirming the presence of gelatin [47]. The FT-IR data of alginate showed main absorption bands at ~3,400 cm^{-1} (-OH vibration) and ~1,050 cm^{-1} (C-O-C vibration). The ~1,400 cm^{-1} peak assigned to the carboxylate symmetric stretching band was clearly observed only in the alginate, while this peak disappeared or decreased in the composite hydrogel [48]. This is

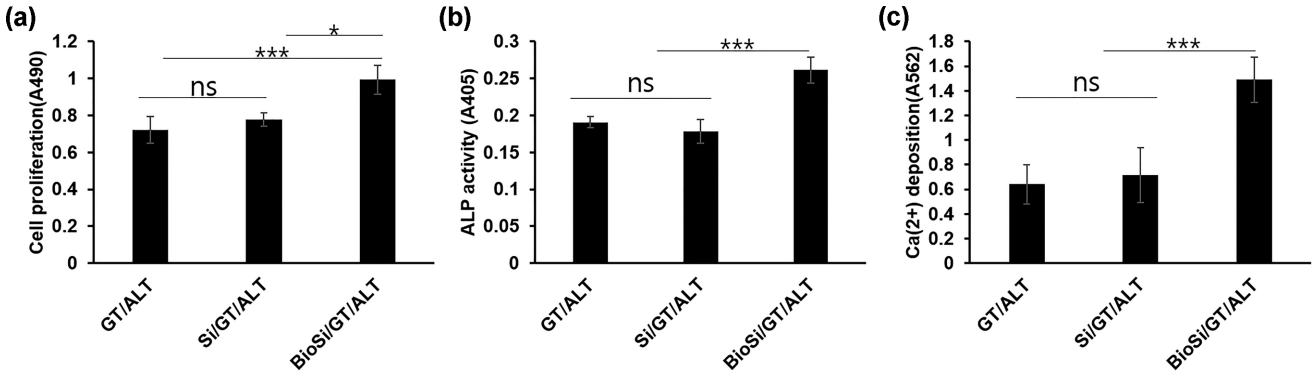

Fig. 6. In vitro osteogenic activity of Biosilica hybrid hydrogel. GT/ALT corresponds to the cross-linked hydrogel of gelatin and alginate via tyramine conjugation; GT/ALT was immersed in silicic acid after being washed and dried, yielding Si/GT/ALT; AqCtLSN-coated GT/ALT was immersed in silicic acid after being washed and dried, yielding BioSi/GT/ALT. The result is expressed as the mean±SD of the three repeated experiment values. (a) Cell proliferation of MC3T3 E1 at Day 7. There was no significant difference (ns) between GT/ALT and Si/GT/ALT. GT/ALT vs BioSi/GT/ALT, ***p<0.001 and Si/GT/ALT vs BioSi/GT/ALT, *p<0.05. (b) Alkaline phosphatase (ALP) activity on Day 14 after osteogenic induction. GT/ALT vs Si/GT/ALT, ns. GT/ALT or Si/GT/ALT vs BioSi/GT/ALT, ***p<0.001. (c) Calcium precipitation on MC3T3 E1 cells on Day 21 after osteogenic induction. GT/ALT vs Si/GT/ALT, ns. GT/ALT or Si/GT/ALT vs BioSi/GT/ALT, ***p<0.001.

because the carboxyl group is involved in the formation of a covalent bond with tyramine via the EDC/NHS reaction and subsequent cross-linking with GT. The absorption peaks of the stretching vibrations of Si-O-Si and Si-OH at ~1,050 cm^{-1} and ~3,400 cm^{-1} [49], respectively, were observed in both silica-containing composites (Si/GT/ALT and Si/AqCtLSN/GT/ALT). These peaks were more enhanced in the AqCtLSN-mediated silica (biosilica)-incorporated composite than in Si/GT/ALT in the absence of this protein. Furthermore, the peak at 800 cm^{-1} corresponded to the Si-O-Si symmetric stretching vibration, and that at 950 cm^{-1} corresponded to the Si-OH bending vibration, which [49] were prominent only in Si/AqCtLSN/GT/ALT (Fig. 5(d)). The FT-IR data showed that silica deposition was more enhanced in the hydrogel immobilized with silica polymerized protein on the surface than the protein-free polymer hydrogel and that the biosilica composite was successfully prepared.

5. *In Vitro* Osteogenic Activity of Biosilica Coated Hydrogel (BioSi/GT/ALT)

The effect of biosilica-coated hydrogels formed by AqCtLSN, designated as BioSi/GT/ALT, on osteo-differentiation was evaluated using MC3T3 E1 mouse preosteoblast. Si/GT/ALT, obtained after 1.5% silicic acid was overlaid on GT/ALT, showed no significant differences between GT/ALT in cell adhesion and proliferation, alkaline phosphatase activity, and calcium deposition activity (Fig. 6). In contrast, BioSi/GT/ALT significantly increased cell adhesion and proliferation, alkaline phosphatase activity, and the degree of calcium precipitation compared to GT/ALT and Si/GT/ALT (Fig. 6). Nature-inspired biosilica is known to promote bone differentiation, particularly when used as a material for hard tissue regeneration. The R5 silica biomineralization domain, derived from diatom-linked recombinant 15mer silk fusion proteins, demonstrated a higher potential to induce silica precipitation and subsequently promote the differentiation of human mesenchymal stem cells (hMSC) [50]. Particularly, because silicatein/biosilica displays osteoinductive properties without osteogenic growth factors, it is considered a promising component for fabricating tissue-engineered scaffolds for bone regeneration [51-54].

CONCLUSION

A novel silica-catalyzing protein derived from *Amphimedon queenslandica* (AqCtLSN) was cloned and expressed heterologously in *E. coli*. AqCtLSN can be produced as a soluble functional protein that is not found in silicatein expression, but its instability owing to its protease activity needs to be further amended. The refolded AqCtLSN from the insoluble form yielded approximately 188 μmoles of silica per mg of AqCtLSN from the silica precursor of TEOS. Furthermore, it exhibited silica deposition activity even after self-assembly and aggregation in a phosphate-containing buffer. This property was utilized to fabricate biosilica-coated composite materials through in situ silicification by coating AqCtLSN on the material. The biosilica composite demonstrated an increased bone cell proliferation, ALP activity, and calcium precipitation compared the case without biosilica. Therefore, AqCtLSN can be utilized both in soluble and aggregated states as a silica-catalyzing agent and, depending on its use, it can be applied to the design of biosilica hybrid materials.

ACKNOWLEDGEMENTS

This work was supported by the National Research Foundation of Korea (NRF) grant funded by the Korean government (MSIT) (NRF-2021R1A5A8032895, NRF-2021R1A2C2011564). This work was also supported by the National Research Foundation of Korea (NRF) funded by the Korea Ministry of Education (NRF-2021 R1I1A3046565). This work was also supported by Korea Environmental Industry & Technology Institute (KEITI) through Project to develop eco-friendly new materials and processing technology derived from wildlife, funded by Korea Ministry of Environment (MOE) (RE202101398).

CONFLICT OF INTEREST

The authors declare that they have no conflict of interest.

REFERENCES

1. L. A. Estroff, *Chem. Rev.*, **108**, 4329 (2008).
2. K. Shimizu, J. Cha, G. D. Stucky and D. E. Morse, *Proc. Natl. Acad. Sci. USA*, **95**, 6234 (1998).
3. M. J. Olszta, D. J. Odom, E. P. Douglas and L. B. Gower, *Connect. Tissue Res.*, **44** Suppl 1, 326 (2003).
4. H. P. Wiesmann, U. Meyer, U. Plate and H. J. Hohling, *Int. Rev. Cytol.*, **242**, 121 (2005).
5. L. B. Gower, *Chem. Rev.*, **108**, 4551 (2008).
6. H. M. Moura and M. M. Unterlass, *Biomimetics* (Basel), **5**, 29 (2020).
7. F. Nudelman and N. A. Sommerdijk, *Angew. Chem. Int. Ed. Engl.*, **51**, 6582 (2012).
8. M. B. Dickerson, K. H. Sandhage and R. R. Naik, *Chem. Rev.*, **108**, 4935 (2008).
9. C. F. Böhm, J. Harris, P. I. Schodder and S. E. Wolf, *Materials*, **12**, 2117 (2019).
10. N. Kroger, R. Deutzmann and M. Sumper, *Science*, **286**, 1129 (1999).
11. M. A. A. Abdelhamid and S. P. Pack, *Acta Biomater.*, **120**, 38 (2021).
12. S. M. Bulatovic, *Handbook of flotation reagents: Chemistry, theory and practice, in Beneficiation of silica sand*, Elsevier, Canada (2015).
13. S. Jafari, H. Derakhshankhah, L. Alaei, A. Fattahi, B. S. Varnamkhasti and A. A. Saboury, *Biomed. Pharmacother.*, **109**, 1100 (2019).
14. Y. Wang, Y. Huang, H. Bai, G. Wang, X. Hu, S. Kumar and R. Min, *Biosensors*, **11**, 472 (2021).
15. S. Kumari, K. H. Min, B. K. Kanth, E. K. Jang and S. P. Pack, *Biotechnol. Bioprocess Eng.*, **25**, 758 (2020).
16. H. Li, X. Chen, D. Shen, F. Wu, R. Pleixats and J. Pan, *Nanoscale*, **13**, 15998 (2021).
17. C. J. Brinker and G. W. Scherer, *Sol-gel science: The physics and chemistry of sol-gel processing*, Academic Press, Boston, London (1990).
18. M. B. Dickerson, R. R. Naik, P. M. Sarosi, G. Agarwal, M. O. Stone K. H. Sandhage, *J. Nanosci. Nanotechnol.*, **5**, 63 (2005).
19. M. J. Limo, A. Sola-Rabada, E. Boix, V. Thota, Z. C. Westcott, V. Puddu and C. C. Perry, *Chem. Rev.*, **118**, 11118 (2018).
20. S. Görlich, A. J. Samuel, R. J. Best, R. Seidel, J. Vacelet, F. K. Leonarski, T. Tomizaki, B. Rellinghaus, D. Pohl and I. Zlotnikov, *Proc. Natl. Acad. Sci. USA*, **117**, 31088 (2020).
21. H. C. Schröder, X. Wang, A. Manfrin, S.-H. Yu, V. A. Grebenjuk, M. Korzhev, M. Wiens, U. Schlossmacher and W. E. G. Müller, *J. Biol. Chem.*, **287**, 22196 (2012).
22. M.-R. Ki, E.-K. Jang and S. P. Pack, *Process Biochem.*, **49**, 95 (2014).
23. A. Krasko, B. Lorenz, R. Batel, H. C. Schroder, I. M. Muller and W. E. Muller, *Eur. J. Biochem,*, **267**, 4878 (2000).
24. W. E. Muller, A. Krasko, G. Le Pennec, R. Steffen, M. Wiens, M. S. Ammar, I. M. Muller and H. C. Schroder, *Prog. Mol. Subcell. Biol.*, **33**, 195 (2003).
25. M. Pozzolini, L. Sturla, C. Cerrano, G. Bavestrello, L. Camardella, A. M. Parodi, F. Raheli, U. Benatti, W. E. Muller and M. Giovine, *Mar. Biotechnol.* (NY), **6**, 594 (2004).
26. X. Wang, H. C. Schröder and W. E. G. Müller, *Trends. Biotechnol.*, **32**, 441 (2014).
27. S. Y. Tabatabaei Dakhili, S. A. Caslin, A. S. Faponle, P. Quayle, S. P. de Visser and L. S. Wong, *Proc. Natl. Acad. Sci. USA*, **114**, E5285 (2017).
28. M. R. Ki, K. B. Yeo and S. P. Pack, *Bioprocess Biosyst. Eng.*, **36**, 643 (2012).
29. H. Oguri, K. Nakashima, K. Godigamuwa, J. Okamoto, Y. Takeda, F. Okazaki, M. Sakono and S. Kawasaki, *J. Biosci. Bioeng.*, **133**, 222 (2022).
30. M. Fairhead, K. A. Johnson, T. Kowatz, S. A. McMahon, L. G. Carter, M. Oke, H. Liu, J. H. Naismith and C. F. van der Walle, *Chem. Commun. (Camb)*, **15**, 1765 (2008).
31. H. Kirschke, A. J. Barrett and N. D. Rawlings, *Lysosomal cysteine proteases*, 2nd Edn., Oxford University Press, Oxford, New York (1998).
32. W. E. Muller, A. Boreiko, X. Wang, S. I. Belikov, M. Wiens, V. A. Grebenjuk, U. Schlossmacher and H. C. Schroder, *Gene*, **395**, 62 (2007).
33. N. V. Povarova, N. A. Barinov, M. S. Baranov, N. M. Markina, A. M. Varizhuk, G. E. Pozmogova, D. V. Klinov, V. B. Kozhemyako and K. A. Lukyanov, *Sci. Rep.*, **8**, 16759 (2018).
34. D. G. Kamenev, Y. N. Shkryl, G. N. Veremeichik, V. A. Golotin, N. N. Naryshkina, Y. O. Timofeeva, S. N. Kovalchuk, I. V. Semiletova and V. P. Bulgakov, *J. Nanosci. Nanotechnol.*, **15**, 10046 (2015).
35. C. L. Fisher and G. K. Pei, *BioTechniques*, **23**, 570 (1997).
36. T. A. Elkhooly, W. E. G. Müller, X. Wang, W. Tremel, S. Isbert and M. Wiens, *Bioinspir. Biomim.*, **9**, 044001 (2014).
37. M. R. Ki, S. H. Kim, T. K. M. Nguyen, R. G. Son, S. H. Jun and S. P. Pack, *ACS Biomater. Sci. Eng.*, (2022). DOI: 10.1021/acsbiomaterials.1c01095.
38. D. K. Lee, M.-R. Ki, E. H. Kim, C.-J. Park, J. J. Ryu, H. S. Jang, S. P. Pack, Y. K. Jo and S. H. Jun, *Biomater. Res.*, **25**, 13 (2021).
39. R. Andre, M. N. Tahir, T. Link, F. D. Jochum, U. Kolb, P. Theato, R. Berger, M. Wiens, H. C. Schroder, W. E. Muller and W. Tremel, *Langmuir*, **27**, 5464 (2011).
40. E.-j. Cheon, S.-H. Kim, D.-K. Lee, Y.-K. Jo, M.-R. Ki, C.-J. Park, H.-S. Jang, J.-S. Ahn, S.-P. Pack and S.-H. Jun, *Biotechnol. Bioprocess Eng.*, **26**, 923, (2021).
41. L. N. Niu, K. Jiao, Y. P. Qi, S. Nikonov, C. K. Yiu, D. D. Arola, S. Q. Gong, A. El-Marakby, M. R. Carrilho, M. W. Hamrick, K. M. Hargreaves, A. Diogenes, J. H. Chen, D. H. Pashley and F. R. Tay, *FASEB J.*, **26**, 4517 (2012).
42. Z. Lipinszki, V. Vernyik, N. Farago, T. Sari, L. G. Puskas, F. R. Blattner, G. Posfai and Z. Gyorfy, *ACS Synth. Biol.*, **7**, 2656 (2018).
43. R. Menard, E. Carmona, S. Takebe, E. Dufour, C. Plouffe, P. Mason and J. S. Mort, *J. Biol. Chem.*, **273**, 4478 (1998).
44. J. D. Bendtsen, H. Nielsen, G. von Heijne and S. Brunak, *J. Mol. Biol.*, **340**, 783 (2004).
45. T. Coradin, A. Coupé and J. Livage, *Colloids Surf. B Biointerfaces*, **29**, 189 (2003).
46. C. J. Oldfield and A. K. Dunker, *Annu. Rev. Biochem.*, **83**, 553 (2014).
47. J. Kozlowska, N. Stachowiak and A. Sionkowska, *Polymers*, **10**, 456 (2018).
48. B.-P. Jiang, L. Zhang, Y. Zhu, X.-C. Shen, S.-C. Ji, X.-Y. Tan, L. Cheng and H. Liang, *J. Mater. Chem. B.*, **3**, 3767 (2015).
49. G. Singh, H. B. Dizaji, H. Puttuswamy and S. Sharma, *Sustainabil-*

ity, **14**, 539 (2022).
50. R. Plowright, N. Dinjaski, S. Zhou, D. J. Belton, D. L. Kaplan and C. C. Perry, *RSC Adv.*, **6**, 21776 (2016).
51. S. Wang, X. Wang, F. G. Draenert, O. Albert, H. C. Schröder, V. Mailänder, G. Mitov and W. E. G. Müller, *Bone*, **67**, 292 (2014).
52. W. E. G. Müller, H. C. Schröder, Q. Feng, U. Schlossmacher, T. Link and X. Wang, *J. Tissue Eng. Regen. Med.*, **9**, E39 (2015).
53. W. Zhu, X. Gao, X. Zou, W. E. G. Müller, S. Wang, Y. Wang and Y. Liu, *J. Biomater Tissue Eng.*, **8**, 258 (2018).
54. O. Dudik, S. Amorim, J. R. Xavier, H. T. Rapp, T. H. Silva, R. A. Pires and R. L. Reis, *Front. Mar. Sci.*, **8**, 637810 (2021).